*Journal of Nano- and Electronic Physics*
Vol. **13** No 6, 06006(4pp) (2021)

*Журнал нано- та електронної фізики*
Том **13** № 6, 06006(4cc) (2021)

# Comparative Study of Thermal and Optical Properties of PANI Based Binary Nanocomposites

Ajay Kumar Sharma*, Manasvi Dixit

*Department of Physics, Swami Keshvanand Institute of Technology, Management & Gramothan, Jaipur 302017, India*

(Received 02 October 2021; revised manuscript received 01 December 2021; published online 20 December 2021)

Nanoscale materials and nanocomposites composed of metals, conducting polymers, carbon nanotubes, because of their optical, mechanical, thermal, and chemical properties, are used in a huge number of applications. Current work includes the fabrication of PANI/rGO, as well as PANI/MWCNT nanocomposites and the study of their optical and thermal characteristics. The article describes in detail the methodology of synthesis and relative optical and thermal study of PANI/MWCNT and PANI/rGO nanocomposites with 8 wt. % rGO/MWCNT in pure PANI using an in-situ chemical oxidation polymerization process. Scanning electron microscopy (SEM) and Fourier Transform Infrared (FTIR) spectroscopy were used to investigate the surface morphology of synthesized nanocomposites. Thermogravimetric analysis (TGA) was used to measure the thermal stability of PANI/rGO and PANI/MWCNT nanocomposites. UV-Visible spectrophotometry studies revealed a decrease in band gap values in specific PANI/rGO (8 wt. %) nanocomposite samples due to the enhanced significant interaction between rGO-doped PANI at molecular conjugation and the corresponding carbon allotropes. The study showed that PANI/rGO specimens have excellent structural, thermal, and optical characteristics, making them suitable for research and development in the field of energy storage devices and their applications.

**Keywords:** Structure of nanoscale materials, Conducting polymers, Electron microscopy, Thermal properties, Optical properties.

DOI: 10.21272/jnep.13(6).06006

PACS numbers: 61.46. – W, 82.35.Cd, 87.64.Ee, 91.60.Ki, 91.60.Mk

## 1. INTRODUCTION

Nanomaterials possess unique physical properties both at the molecular and macro scales, opening up new possibilities for physicochemical and biomedical studies and applications in a variety of fields of chemistry, genetics, and medicine. Contemporary developments necessitate the creation of innovative products with unique properties. In recent decades, numerous attempts have been conducted to develop nanomaterials with specific functions using new nanoscience and nanotechnology expertise.

Doping with carbon nanocomposites of polymer structures, particularly for preparing electronic and optical materials, is also an important research field. Standard conducting polymers can be used as matrices in practical composite planning. These products can be utilized to achieve various applications, including data storage, photovoltaic cells and photodiodes, optical limits, photosensitive print drums, and most often due to the integration of complementary CNTs with specific properties of polymers. Polymer nanocomposite materials have emerged as a critical field of study in contemporary science and technology [1]. With the increased need for electricity and refining fuels over the last decades, energy storage has been a critical element in economic development. Commercially, energy storage systems are classified into mechanical (flywheel system for storing energy, compressed air energy storage systems, and hydroelectric energy storage systems), electromagnetic (capacitor, inductor, supercapacitor, and superconducting magnetic energy storage systems), chemical (biofuels, hydrogen, and liquid nitrogen), and biological energy storage systems [2-5]. In light of the expanding range of appliances, the optimal method and energy storage unit, which fully meet economic and technological requirements, are still inaccessible. Nanoparticles or nanocomposites composed of metals, polymers, semiconductors or oxides are of particular interest and are used as quantum dots and chemical catalysts due to their electrical, optical, thermal and a variety of many other characteristics. Carbon atoms in conjugated polymers have alternating single and double bonds. Each bond includes a strong, localized sigma bond that holds the polymer together, as well as a weaker, localized $\pi$-bond. These unsaturated $\pi$-bonded polymers have low ionization potentials and strong electron affinities, facilitating oxidation-reduction reactions.

Thus, the electrical structure of conjugated polymers is radically distinct, with one vacant electron ($\pi$-electron) in a single carbon atom due to chemical bonding. The overlap of $\pi$-orbitals containing consecutive atoms of carbon in the polymer backbone results in relocation of electrons along the polymer backbone. This relocation of electrons creates a path for charge mobility around the polymer chain backbone. Thus, the electrical composition of conducting polymers is defined as chain symmetry, i.e., the number and type of atoms inside a repeating unit, resulting in semiconducting or even metallic properties for these polymers.

In this work, we chose nanoparticles of reduced graphene oxide (rGO) and multiwall carbon nanotubes (MWCNT), which are utilized to create nanocomposites from polymers with polyaniline (PANI). PANI composites with GO and rGO also represent a viable candidate for this application, among which rGO is preferred due

* ajaymnit19@gmail.com

 

to its higher conductivity and thermal stability as compared to rGO. PANI has become widely known in the last decade due to the inclusion of energetic –NH– groups in polymer chains, interesting oxidation properties, low-cost monomers, cold amalgamation and high electrical conductivity. PANI has attracted the attention of researchers owing to its peculiar electrical properties; nevertheless, PANI tends to agglomerate in organic solvents, which reduces its processability [6, 7]. Carbon nanocomposites such as rGO and MWCNT have a high percolation threshold and low abundance. Carbon nanocomposites are often used as fillers in PANI matrix components to improve their optical and thermal stability.

## 2. EXPERIMENTAL DETAILS

PANI/MWCNT(8 wt. %) and PANI/rGO(8 wt. %) nanocomposites were created by using ammonium peroxide sulphate (APS) as an oxidant and in-situ aniline polymerization by chemical oxidation in the presence of rGO and MWCNT nanoparticles at temperatures ranging from 0 to 5 °C in the presence of air. The rGO and MWCNT nanoparticles remained suspended in a 1 M HCl solution for one hour after being sonicated to avoid aggregation of nanoparticles. Before being sonicated for 30 min, 0.1 M aniline solution was dissolved in 100 ml of 1 M HCl solution with 10 ml rGO and MWCNT nanoparticles in order to get the desired result. After 2 h of continuous stirring at 0-5 °C, 100 ml of a 1 M HCl mixture containing APS [$(NH_4)_2S_2O_8$)] in an equivalent aniline molar ratio were gradually added to the suspension solution by a drop-by-drop method, resulting in improved dispersion after addition of APS. To complete the chemical reaction, the mixture was kept at rest overnight. The reaction's precipitate was drained out, washed several times with 1 M HCl, and dried under vacuum for 24 h [8, 9]. As a result, the nanocomposite powder was prepared in the form of conductive emerald salt (ES) of PANI/MWCNT(8 wt. %) and PANI/rGO (8 wt. %) nanocomposites.

Scanning electron microscopy (SEM) using FE-SEM (FEI quanta 450) was performed to examine the surface morphology of the produced nanocomposites. Nanocomposites were characterized using Fourier transform infrared spectroscopy (FTIR). A Perkin Elmer FTIR spectrophotometer was used to record the FTIR spectra in the region of 4000 to 500 $cm^{-1}$. The UV-Vis absorption spectra were recorded using a Perkin Elmer LAMBDA 750 UV-Vis-NIR spectrophotometer. Thermogravimetric analysis (Perkin Elmer STA 6000) was used to determine the material's thermal stability under consideration.

## 3. RESULTS AND DISCUSSION

### 3.1 Structural Characterization

Fig. 1a shows the SEM image of pure PANI, which exhibits a relatively plane surface, indicating rough protuberances in the layered structure with cracks, while Fig. 1b and Fig. 1c show the SEM images of the nanocomposite structure. SEM micrographs do not show any significant changes in PANI/MWCNT composites, except some irregular lumps and smoothed boundaries of dispersed MWCNT within the PANI matrix. It is also observed that agglomeration of MWCNT takes place, which strongly affects the morphology of the base matrix of the PANI molecule. Apart from the distribution of uneven lumps and smoothed boundaries, no significant changes were observed in the SEM images of composites. Further, the absence of the rGO structure on the surface indicates the encapsulation of the rGO structure by PANI polymer chains [10].

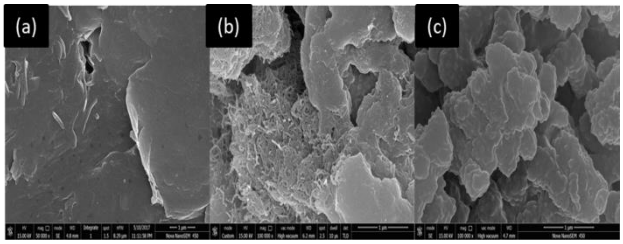


**Fig. 1** – SEM pictures of (a) PANI, (b) PANI/MWCNT (8 wt. %), (c) PANI/rGO(8 wt. %)

Fig. 2 depicts the FTIR spectra of PANI and its MWCNT/rGO nanocomposites. FTIR spectra of PANI reveal its characteristic peaks at 3423, 1628, 1133, and 607 $cm^{-1}$, as well as the C=C stretching peak of "quinonoid" (1628 $cm^{-1}$), N–H stretching vibration peak (3423 $cm^{-1}$), and N=Q=N stretching peak (1133 $cm^{-1}$), [11] all of which are visible in the spectrum.

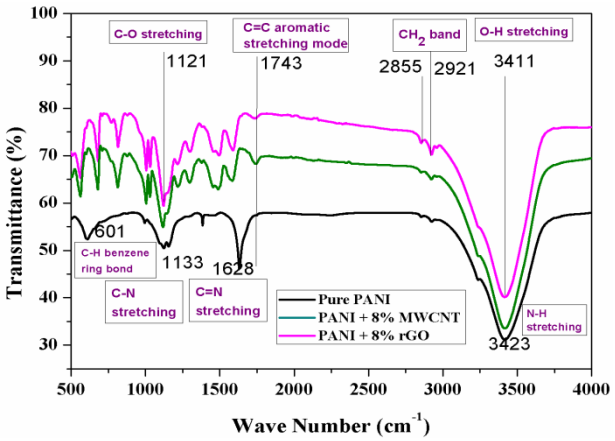


**Fig. 2** – FTIR spectra of pure PANI and nanocomposites

In addition, some peaks were detected, such as 3411 $cm^{-1}$, which is attributed to absorbed water and O–H stretching mode of carboxyl groups in MWCNT/rGO, dual peaks at 2855 and 2921 $cm^{-1}$, which are credited to C–H stretching in $CH_2$ and $CH_3$ groups, respectively, and dual peaks at 2855 and 2921 $cm^{-1}$, indicating the development of a strong interaction amongst the conjugated construction of "quinoid rings of PANI" and $\pi$-bonded MWCNT/rGO surfaces of the composite structure [12, 13].

### 3.2 Thermal Stability Analysis

Thermal studies were done using thermogravimetric analysis (TGA) scans from room temperature to 900 °C. Fig. 3 shows the deviation of weight loss relative to temperature for PANI and its MWCNT/rGO nanocomposites due to the decomposition of water and oxygen containing groups of MWCNT/rGO nanocompo-

sites. It was found that, first, at a marginally greater room temperature, the tendency for weight loss for PANI/MWCNT (8 wt. %) and PANI/rGO(8 wt. %) nanocomposites is higher. This procedure remains with the continuing increase in temperature. The weight loss for PANI/rGO and PANI/MWCNT nanocomposites suddenly decreases within 250 to 350 °C temperature range due to the destruction of PANI chain fragments [14]. Fig. 3 also shows that at higher temperatures, the comparative weight loss of the PANI base matrix dispersed with MWCNT(8 wt. %) and rGO(8 wt. %) nanocomposites is smaller in comparison to pure PANI. Definitely, the main weight loss of PANI containing 8 % MWCNT is 57.96 % and that containing 8 % rGO is 50.85 % relative to 62.11 % PANI at 900 °C to achieve significant thermal stability associated with PANI. This shows that the thermal stability of PANI/rGO (8 wt. %) is improved compared with PANI/MWCNT (8 wt. %) nanocomposite.

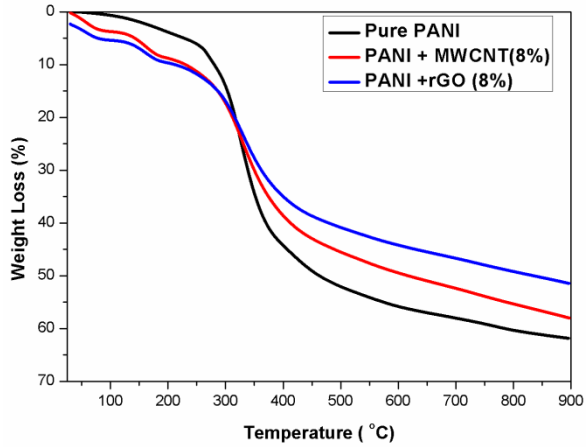


**Fig. 3** – TGA analysis of PANI, PANI/MWCNT and PANI/rGO nanocomposites

### 3.3 Optical Band Gap Analysis

Fig. 4 depicts the Tauc's plot of pure PANI, PANI/MWCNT(8 wt. %) and PANI/rGO(8 wt. %) nanocomposites. According to Tauc's model, the optical band gap can be calculated from UV-Vis spectra by applying the relationship given in equation (1) [15]:

$$\alpha h\nu = A\left(h\nu - E_g\right)^n, \qquad (1)$$

where $E_g$ is the band gap of the material (it may be direct band gap or indirect band gap), $\nu$ is the frequency of incident rays, $\alpha$ is the absorption coefficient, $h$ is the Planck constant, $A$ is an arbitrary constant. The value of $n$ is 2 for an indirect electron transition or 1/2 for a direct transition.

The Tauc's plot displays the determination of the band gap for PANI, PANI/MWCNT(8 wt. %) and PANI/rGO(8 wt. %) nanocomposites. The band gap of PANI is observed at 3.40 eV, which is similar to other reports [16]. A decrease in the band gap with the addition of MWCNT/rGO is also observed from 3.40 to 3.20 eV with 8 wt. % MWCNT, and from 3.40 to 3.18 eV with 8 wt. % rGO, which indicates an adequate effect of complex coordination between PANI molecular chain segments doped with MWCNT/rGO nanoparticles.

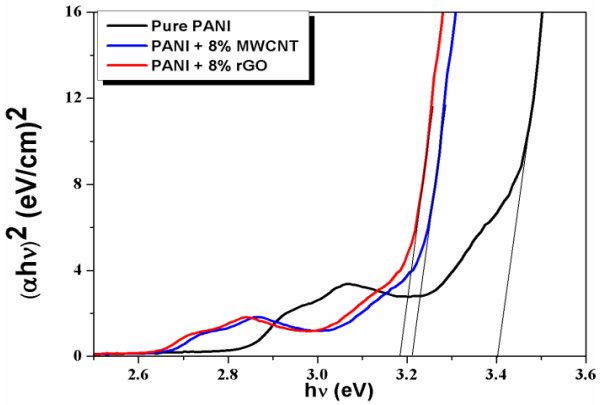


**Fig. 4** – $(ah\nu)^2$ versus $h\nu$ plot for PANI and nanocomposites

The change in the band gap indicates modified absorption of the coordination complex formed between MWCNT/rGO and PANI chains, which exhibit a decreasing trend due to MWCNT/rGO nanoparticles in nanocomposites [17, 18]. The charge transfer from MWCNT/rGO to polymer chains causes a decrease in the band gap because new excitation energy levels are created below the regular band gap [19, 20].

## 4. CONCLUSIONS

The study of the structural and thermal stability of a specially prepared PANI base matrix dispersed with MWCNT(8 wt. %) and rGO(8 wt. %) nanocomposites allows to draw the following conclusions.

1. SEM and FTIR studies reveal that the overall morphology of MWCNT and rGO doped PANI specimens has improved.

2. TGA analysis of these nanocomposites shows better thermal stability of PANI/rGO(8 wt. %) nanocomposite in comparison with pure PANI and PANI/MWCNT (8 wt. %) studied sample. This shows that the addition of rGO to the PANI matrix increases the thermal stability of nanocomposites. The TGA findings show that covalent bonds were established between PANI and rGO functional groups, resulting in improved thermal stability of nanocomposites.

3. Optical study of nanocomposites reveals that the distribution of MWCNT and rGO offers a more appropriate band gap reduction to 5.88 % and 6.47 % due to the interaction between $\pi$-$\pi^*$ transition PANI in molecular conjugation and carbon allotropes (MWCNT and rGO) in the composite. The reason for the bond shift is related to the new excitation energy levels created by MWCNT/rGO near the band gap of the pure PANI.

Finally, the study found that PANI/rGO specimens show superior structural, thermal, and optical characteristics, making them suitable for research and development in the design and application of energy-efficient supercapacitors.

## REFERENCES


1. N.A. Kotov, *Nature* **442** No 7100, 254 (2006).
2. S.S. Siwal, Q. Zhang, N. Devi, V.K. Thakur, *Polymers (Basel)* **12** No 3, 505 (2020).
3. A.T. Smith, A.M. LaChance, S. Zeng, B. Liu, L. Sun, *Nano Mater. Sci.* **1** No 1, 31 (2019).
4. R. Singh, R.B. Choudhary, *Optik (Stuttg)* **127** No 23, 11398 (2016).
5. J. Liu, X. Zhao, J. Zang, C. Cao, Y. Feng, *Sci. Rep.* **4** 6492 (2014).
6. J. Zhu, H. Gu, Zh. Luo, N. Haldolaarachige, D.P. Young, S. Wei, Zh. Guo, *Langmuir* **28** No 27, 10246 (2012).
7. S. Virji, J. Huang, R.B. Kaner, B.H. Weiller, *Nano Lett.* **4** No 3, 491 (2004).
8. S. Srivastava, S.S. Sharma, S. Kumar, S. Agrawal, M. Singh, Y.K. Vijay, *Int. J. Hydrogen Energy* **34** No 19, 8444 (2009).
9. S.G. Bachhav, D.R. Patil, *Am. J. Mater. Sci.* **5** No 4, 90 (2015).
10. S. Dhibar, C.K. Das, *Ind. Eng. Chem. Res.* **53** No 9, 3495 (2014).
11. R. Sainz, W.R. Small, N.A. Young, C. Vallés, A.M. Benito, W.K. Maser, Marc in het Panhuis, *Macromolecules* **39** No 21, 7324 (2006).
12. H. Fan, H. Wang, N. Zhao, X. Zhang, J. Xu, *J. Mater. Chem.* **22** No 6, 2774 (2012).
13. F. Avilés, J.V. Cauich-Rodríguez, L. Moo-Tah, A. May-Pat, R. Vargas-Coronado, *Carbon* **47** No 13, 2970 (2009).
14. X.-Z. Tang, W. Li, Z.-Z. Yu, M.A. Rafiee, J. Rafiee, F. Yavari, N. Koratkar, *Carbon* **49** No 4, 1258 (2011).
15. K. Vadiraj, S. Belagali, *IOSR J. Appl. Chem.* **8** No 1, 53 (2015).
16. M. Mitra, C. Kulsi, K. Chatterjee, K. Kargupta, S. Ganguly, D. Banerjee, S. Goswami, *RSC Adv.* **5** No 39, 31039 (2015).
17. X. Li, G. Wang, X. Li, D. Lu, *Appl. Surf. Sci.* **229** No 1-4, 395 (2004).
18. R. Cruz-Silva, J. Romero-Garcıa, J.L. Angulo-Sanchez, E. Flores-Loyola, M.H. Farıas, F.F. Castillon, J.A. Dıaz, *Polymer (Guildf)* **45** No 14, 4711 (2004).
19. M.J. Almasi, T. Fanaei Sheikholeslami, M.R. Naghdi, *Compos. Part B Eng.* **96**, 63 (2016).
20. A.K. Sharma, P.K. Jain, R. Vyas, V. Mathur, V.K. Jain, *Mater. Today: Proc.* **38**, 1214 (2021).


## Порівняльне дослідження теплових та оптичних властивостей бінарних нанокомпозитів на основі PANI


Ajay Kumar Sharma, Manasvi Dixit

*Department of Physics, Swami Keshvanand Institute of Technology, Management & Gramothan, Jaipur 302017, India*



Нанорозмірні матеріали та нанокомпозити, які складаються з металів, провідних полімерів, вуглецевих нанотрубок, використовуються у величезній кількості додатків завдяки своїм оптичним, механічним, тепловим та хімічним властивостям. Робота полягає у виготовленні нанокомпозитів PANI/rGO і PANI/MWCNT та вивченні їх оптичних і теплових характеристик. У статті детально описано методологію синтезу та відповідне оптично-теплове дослідження нанокомпозитів PANI/rGO та PANI/MWCNT з 8 ваг. % rGO/MWCNT у чистому PANI з використанням процесу хімічної окислювальної полімеризації in-situ. Для дослідження морфології поверхні синтезованих нанокомпозитів були використані скануюча електронна мікроскопія (SEM) та інфрачервона спектроскопія з перетворенням Фур'є (FTIR). Для вимірювання теплової стабільності нанокомпозитів PANI/rGO і PANI/MWCNT використовували термогравіметричний аналіз (TGA). Дослідження спектрофотометрії в УФ та видимій областях спектру виявили зменшення значень ширини забороненої зони в конкретних нанокомпозитних зразках PANI/rGO (8 wt. %) через посилення взаємодії між rGO-легованим PANI при молекулярному з'єднанні та відповідними алотропами вуглецю. Дослідження показало, що зразки PANI/rGO мають чудові структурні, теплові та оптичні характеристики, що робить їх придатними для досліджень і розробок у сфері накопичувачів енергії та її додатків.



**Ключові слова:** Структура нанорозмірних матеріалів, Провідні полімери, Електронна мікроскопія, Теплові властивості, Оптичні властивості.